Laboratory Studies of Bromide Oxidation in the Presence of Ozone: Evidence for a Glass-Surface Mediated Reaction

CORT ANASTASIO* and MICHAEL MOZURKEWICH
Department of Chemistry and Centre for Atmospheric Chemistry, York University, 4700 Keele Street, North York, Ontario M3J 1P3, Canada

Abstract. The reaction of sodium bromide particles in the presence of ozone was studied in a flow system both under dark conditions and with 254 nm radiation. We found that there was significant formation of gaseous bromine (probably Br_2) in the presence of ozone in the dark, and that bromide deposited to the walls of the Pyrex reaction flask was its source. The observed rate of gaseous bromine formation in these experiments was approximately 100–1000 times faster than expected based on the known rate constant for aqueous reaction of bromide with ozone. While the mechanism responsible for this enhanced reactivity was not identified, based on previous reports we suggest that the glass surface converted ozone to more reactive species, such as hydroxyl radical, which in turn oxidized bromide. In the presence of 254 nm radiation, rates of gaseous bromine collection were further enhanced, likely as a result of increased radical production in the system, and wall-deposited bromide was also the source of the gaseous bromine. In these 'light' experiments, there was a significant decline in ozone mixing ratios, consistent with bromine radical chemistry. These results suggest the possibility that ozone reacting with internally mixed silicate/sea-salt particles might be a significant mechanism for the oxidation of particulate halides, and subsequent release of photoactive halogen species, in the marine boundary layer.

Key words: aerosol chemistry, aqueous-phase chemistry, bromide, marine boundary layer, ozone.

1. Introduction

Recent field campaigns have shown that there can be significant amounts of reactive halogen species and halogen radicals in the marine boundary layer (MBL) in both mid-latitudes and polar regions. For example, reactive chlorine gases, including Cl_2, have been measured in the mid-latitude MBL (Keene *et al.*, 1993; Pszenny *et al.*, 1993; Spicer *et al.*, 1998), while photoactive halogens such as Br_2 and BrCl have been measured in the Arctic MBL before and after Polar Sunrise (Impey *et al.*, 1997; Foster *et al.*, 2001). Photolysis of these reactive halogens produces $Br^{\bullet}$ and $Cl^{\bullet}$ radicals, which have been detected indirectly via measurements of hydrocarbon

* Current address: Atmospheric Science Program, Department of Land, Air and Water Resources, University of California, One Shields Avenue, Davis, CA 95616-8627, U.S.A.,
e-mail: canastasio@ucdavis.edu

decays (Finlayson-Pitts, 1993; Jobson *et al.*, 1994) and by detection of secondary radicals such as $BrO^{\bullet}$ (e.g., Hausmann and Platt, 1994; Richter *et al.*, 1998). In addition, field measurements have shown that $IO^{\bullet}$ is also commonly present in the remote MBL (Allan *et al.*, 2000).

Halogen radicals can have significant effects upon the chemistry of the marine boundary layer. For example, $Br^{\bullet}$ is largely responsible for the episodes of complete or near-complete destruction of tropospheric ozone observed during the Arctic spring (Jobson *et al.*, 1994; Michalowski *et al.*, 2000). Similarly, computer models suggest that bromine radicals can also lead to ozone destruction in the mid-latitude MBL (Sander and Crutzen, 1996; Vogt *et al.*, 1996), while chlorine radicals can either create or destroy tropospheric ozone, depending upon the mixing ratio of NO_x (Pszenny *et al.*, 1993). Model results indicate that iodine radicals can also lead to destruction of ozone, both through direct reactions in the gas phase as well as by enhancing the release of reactive bromine and chlorine species from marine aerosol particles (Vogt *et al.*, 1999; McFiggans *et al.*, 2000). In addition to their effects on ozone, bromine and chlorine radicals can also react with hydrocarbons and dimethylsulfide in the MBL (Keene *et al.*, 1996; Sander and Crutzen, 1996; Vogt *et al.*, 1996; De Haan *et al.*, 1999).

The formation of reactive bromine species, such as Br_2, appears to be initiated by the oxidation of sea-salt bromide (either in sea-salt particles, sea-ice, or on the snowpack), followed by multiphase propagation reactions. One possible initiation reaction is the aqueous oxidation of bromide by ozone to form HOBr (von Gunten and Hoigné, 1994; Disselkamp *et al.*, 1999)

$$O_3(aq) + Br^- \rightarrow OBr^- + O_2(aq) \tag{R1}$$

$$OBr^- + H^+ \rightarrow HOBr(aq)\,. \tag{R2}$$

The HOBr formed can then participate in a propagation reaction with aqueous bromide to form molecular bromine via (Fan and Jacob, 1992)

$$HOBr(aq) + Br^- + H^+ \rightarrow Br_2(aq) + H_2O(l)\,. \tag{R3}$$

In sea-salt particles or sea ice, the following propagation sequence is thought to be more important, given the high molar ratio of Cl^- to Br^- (Vogt *et al.*, 1996; Oum *et al.*, 1998a)

$$HOBr(aq) + Cl^- + H^+ \rightarrow BrCl(aq) + H_2O(l) \tag{R4}$$

$$BrCl(aq) + Br^- \rightarrow Br_2(aq) + Cl^-\,. \tag{R5}$$

Laboratory experiments have shown that Br_2 is formed from the reaction of ozone with both deliquesced sodium bromide particles (DeHann *et al.*, 1999) and frozen seawater (Oum *et al.*, 1998a). The formation of Br_2 has also been observed during ozone exposure of solid NaBr, and mixtures of solid NaBr and NaCl, at

room temperature in the presence of water vapor (Hirokawa *et al.*, 1998). However, based on the reported rate constant for R1 in aqueous solution (160 M^{-1} s^{-1}; Hoigné *et al.*, 1985), reaction (R1) appears to be too slow to be an important initiation step in aqueous sea-salt particles in mid-latitudes. A number of other initiation mechanisms have also been proposed, including reactions of bromide with NO_y species such as N_2O_5 or $NO_3^{\cdot}$ (Laux *et al.*, 1994; Sander and Crutzen, 1996), hydroxyl radical (Mozurkewich, 1995), and peroxymonosulfuric acid (Mozurkewich, 1995), but it is unclear how important these mechanisms are in different regions of the MBL. The Br_2 and BrCl produced in the above sequences can evaporate to the gas phase and photolyze to produce $Br^{\cdot}$ and/or $Cl^{\cdot}$. Reaction of $Br^{\cdot}$ with ozone in the gas phase can then lead to production of HOBr

$$Br^{\cdot}(g) + O_3(g) \rightarrow BrO^{\cdot}(g) \quad \text{(R6)}$$

$$BrO^{\cdot}(g) + HO_2^{\cdot}(g) \rightarrow HOBr(g) \quad \text{(R7)}$$

which can partition back to sea-salt and continue the cycles described above.

While there is still uncertainty in the mechanisms for formation of reactive bromine species, especially in the initiation steps, it is even less clear how reactive chlorine gases such as HOCl and Cl_2 are produced in the MBL. Available evidence suggests that Cl_2 can be formed from the reaction of hydroxyl radical ($^{\cdot}OH$) with chloride on sea-salt particles (Behnke *et al.*, 1995; Oum *et al.*, 1998b), possibly as a result of a surface-enhanced reaction (Knipping *et al.*, 2000). In contrast, iodine chemistry in the MBL appears to be relatively well-understood. According to current models, $I^{\cdot}$ radicals are formed via photolysis of gas phase biogenic iodocarbon species and subsequent propagation and termination reactions occur both in the gas and particle phases (Vogt *et al.*, 1999; McFiggans *et al.*, 2000).

Our initial goal in this work was to experimentally investigate the importance of hydroxyl radical as an oxidant for Br^- in aqueous particles. However, after starting these experiments, we found that the reaction of ozone with bromide in the dark appeared to proceed much more rapidly than predicted based on known rate constants in bulk aqueous solution. Given the potentially important environmental implications of this observation, we then focused on this ozone chemistry. The results from this investigation of ozone oxidation of bromide are described here.

2. Experimental

2.1. MATERIALS

All chemicals were obtained from BDH and were reagent grade or better; sodium bromide was assurance grade. The water used was first treated with reverse osmosis and then distilled in glass with added $KMnO_4$; concentrations of Mn in this distilled water were below detection limits (<0.7 μM). The air used was from an Aadco 737-12A air purifier. For most experiments (those after experiment #20), the Aadco

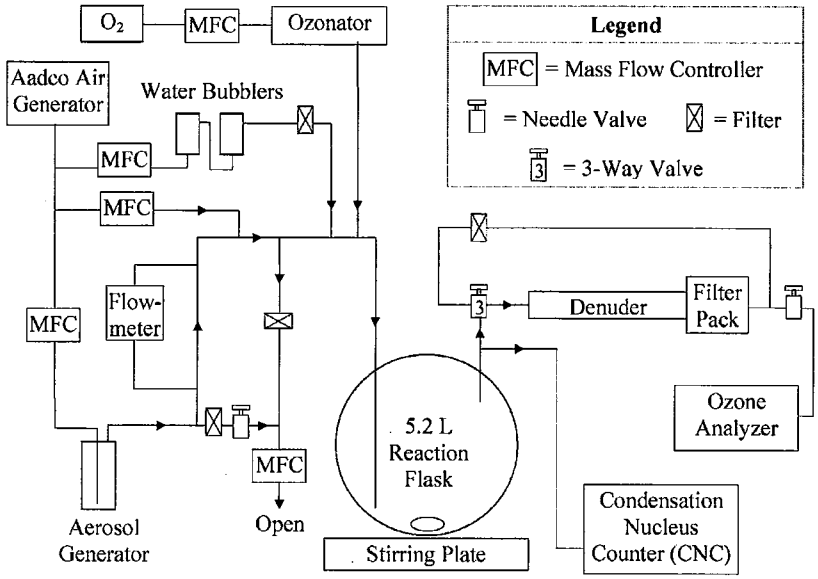

Figure 1. Experimental apparatus used in this study. Arrows indicate direction of flow during an experiment.

air was scrubbed to remove NO_x by passing it through CrO_3 (to oxidize NO to NO_2) and then soda lime (to remove NO_2).

2.2. AEROSOL REACTION SYSTEM

The aerosol reaction system used for experiments is illustrated in Figure 1. NaBr particles were generated by running air at 1.20 slpm (standard liter per minute at 0 °C and 1 atm) through a 1-jet Collison nebulizer (BGI, Inc.) containing 0.100% NaBr. In order to dilute the resulting aerosol, the bulk of this flow was discarded and only 0.10–0.15 slpm (determined by measuring the pressure drop across a length of tubing) was sent downstream towards the reaction flask. This aerosol flow was then diluted with 2.00 slpm of dry air and split, with approximately 0.4 slpm going towards the reaction flask and 1.7 slpm being discarded. The 0.4 slpm aerosol flow was then diluted with 2.0 slpm of humidified air (air passed through two water bubblers in series) and mixed with 0.020 slpm of ozone in O_2 (0.020 slpm of O_2 only in 'blank' experiments). The resulting final flow of 2.42 slpm typically had a particle number concentration (N) of 2.0×10^4 cm^{-3} (typical aerosol mass of 13–18 $\mu g\ m^{-3}$), a relative humidity of 70%, and an ozone mixing ratio between 0–1000 ppbv. Ozone was made by passing either oxygen (>99.6%, extra dry, Matheson; experiments 18–41) or Aadco air (experiments 1–18) through a Thermo Environmental 49-003 UV-light ozone generator/analyzer.

The 2.42 slpm flow of particles, water vapor, and O_3 was sent to a cleaned 5.2 L, 4-neck, borosilicate glass reaction flask (Pyrex, Ace 6954-89) containing a quartz immersion well in the center neck. The residence time of the reaction mixture in the flask was approximately 2 minutes. The flask was rapidly stirred using a Teflon-coated stirring bar; based on visual observations of aerosol made from a 5% NaBr solution, the flask was well-mixed in approximately 10 s. For experiments carried out in the dark, the flask and other reactor components were covered with aluminum foil. For experiments that used UV light, an air-cooled 5 W Hg Analamp (BHK 80-1025-01) was inserted into the quartz immersion well. The flask was not covered with foil in these light experiments. The temperature of the reaction flask was monitored with a mercury thermometer inserted into one of the flask necks. Temperatures in the flask were 25–28 °C for dark experiments and 30–31 °C for light experiments. The pressure immediately upstream of the reaction flask was measured using a Magnehelic gauge (Dwyer, 2000-10 kPa), and was always $\leqslant$3.7 kPa above ambient.

Approximately 11% of the flow out of the reaction flask ($\approx$ 0.27 slpm) was sent to a TSI 3020 condensation nucleus counter to measure particle number concentrations. Using a 3-way valve (Swagelok SS-43XS4), the remainder of the flow was either (i) sent to the denuder/filter pack (DFP) for collection or (ii) shunted around the DFP (before and after collection). In a typical experiment, the water bubblers were filled first (typical $t \sim -100$ min, i.e., 100 min prior to collection on the DFP), the nebulizer was filled with NaBr solution ($t \sim -15$ min), the line from the ozonator was connected ($t \sim -6$ min; note that the ozonator had previously been turned on and had already stabilized), and the flow was diverted from the shunt to the DFP ($t = 0$). This procedure allowed the system components to reach steady state prior to collection of material in the DFP.

The DFP was composed of one glass annular denuder (242 mm L, 1 mm annular space; URG-2000-30B) to collect gaseous bromine compounds, followed by a Teflon filter pack to collect particles. Prior to use, denuders were coated with a 1% Na_2CO_3 solution and then dried with Aadco air. The Teflon filter pack held three 47 mm diameter filters in series: a Gelman Zefluor membrane (2 μm pore size) to collect particles, followed by two KOH-impregnated Whatman 41 filters to collect any gaseous bromine volatilized from the Zefluor.

The relative humidity (RH) of the reaction stream was measured downstream of the DFP with a Vaisala Humitter 50U probe (calibrated using an EG& G Dew-All dew point instrument) connected to an Electronumerics Micro-P readout. Ozone concentrations were measured downstream of this with a Thermo-Environmental Instruments 49-003 ozone generator/analyzer (fitted with an O_3 scrubber from Amko, Z-0284-A) that was calibrated using a calibrated Dasibi 1003-RS from the Ontario Ministry of the Environment. NO_y concentrations were measured prior to most experiments by putting the combined flow from the Aadco air generator and ozonator into a Thermo Environmental 42S NO_x analyzer; for most experiments NO_y mixing ratios were <200 pptv (average $\pm$1 standard deviation = 110 $\pm$ 70

Table I. Ozone exposure experiments in the dark (T = 25–28 °C)[a]

Expt. #	N (cm^{-3})	O_3 (ppbv)	NO_y[b] (ppbv)	Pre-load Time[c] (min)	Denuder Time[d] (min)	$R_{Br(w)}$[e] ($\mu g\ hr^{-1}$)	D{Br(p)}[f] (μg)	D{Br(g)}[g] (μg)	$R_{Br(g)}$[h] ($\mu g\ hr^{-1}$)	$k_{W,OX}$[i] (hr^{-1})	$\frac{k_{W,OX}}{k'_{O_3}}$[j]
7	2×10^7	1050	~1	65	300	[48]	27	29	5.8	[0.017]	[2.4]
12	2.0×10^5	950	~1	170	120	–	2.1	6.1	3.0	–	–
16[k]	1.4×10^4	880	>1[k]	248	180	[0.85]	1.1	3.4	1.1	[0.14]	[26]
20	2.3×10^4	890	1	284	180	[1.4]	0.46	2.8	0.92	[0.058]	[10]
23	2.3×10^4	810	0.3	167	120	[1.4]	0.54	1.9	0.93	[0.098]	[20]
27	1.8×10^4	210	0.1	18	280	0.87	0.54	2.3	0.50	0.13	100
29[l]	1.8×10^4	210	0.1	19	180	1.4	0.68	2.6	0.88	0.22	160
31	2.0×10^4	29	0.17	25	180	1.2	0.82	2.4	0.80	0.22	1200
32[m]	2.0×10^4	32	0.12	23	180	1.3	0.82	0.97	0.32	0.071	350
33	2.0×10^4	220	0.15	22	180	1.5	0.82	2.9	0.95	0.22	160
34–37[n]	2.0×10^4	220	0.13	19	60–280	1.4	1.8	3.8	0.81	0.15	110
39[o]	$2.0 \times 10^4/0$[o]	230	0.15	122	123	0.95/0[o]	0.00	1.1	0.52	0.16	110
40	2.0×10^4	230	0.19	126	120	1.1	0.78	2.1	1.0	0.18	120

[a] Experiments not listed were either ozone experiments with light (Table III), blank (air) experiments, or denuder and filter blanks. Values in square brackets were either estimated (based on values in similar experiments) or calculated using at least one estimated quantity.

[b] Mixing ratio of NO_y measured in the combined air stream from the Aadco generator and ozonator prior to the experiment.

[c] Amount of time that NaBr particles were sent to the reaction flask prior to beginning ozone exposure.

[d] Amount of time that outflow from the reactor was collected on the denuder.

[e] Rate of deposition of NaBr particles onto the walls of the flask. Values for experiments 16, 20, and 23 were not measured and were estimated from the average value for $R_{Br(w)}$ from the other $N \approx 2 \times 10^4\ cm^{-3}$ experiments ($1.2\ \mu g\ hr^{-1}$ at $2.0 \times 10^4\ cm^{-3}$), taking into account differences in particle number concentration. The value for experiment 7 was taken from the corresponding blank experiment.

[f] Mass of particulate bromide collected on the denuder during the experiment, corrected for amount of flow sent to the CNC.

[g] Mass of gaseous bromine collected on the denuder during the experiment, corrected for the flow sent to the CNC (see Equation (1)). The relative standard deviation for D{Br(g)} was ±31–35%.

[h] Rate of collection of gas-phase bromine on the denuder (see Equation (2)). The relative standard deviation for $R_{Br(g)}$ was ±31–35% except for experiment 39 (±5%).

[i] Apparent first-order rate constant for oxidation of bromide deposited to the flask walls (see Equation (A6)). Relative standard deviations for $k_{W,OX}$ were typically ±40% except for experiments 16, 20, and 23 (±50%) and experiment 39 (±5%).

[j] Ratio of experimentally determined rate constant for oxidation of deposited bromide to the pseudo-first order rate constant for bromide oxidation expected based on the aqueous reaction of bromide with ozone.

[k] It was later determined that the timer in the Aadco air purifier was broken during this experiment. Therefore the resulting air stream for this experiment (and for experiment #17; see Table III) was not as clean as during other times.

[l] Air from a cylinder (Zero Grade, ~360 ppmv CO_2, Matheson) was used in place of Aadco air.

[m] High purity nitrogen (< 1 ppm O_2, Matheson) was used in place of Aadco air. The partial pressure of O_2 in this experiment was calculated to be 0.83%; this is 26 times lower than p_{O_2} in the other experiments (21.6%).

[n] Four separate denuders were collected during the course of this experiment. The results are plotted in Figure 3.

[o] The reactor was first pre-loaded with NaBr particles for 122 minutes (in the absence of ozone), then the flow of particles was stopped and the reactor was exposed to O_3 for 123 minutes.

pptv), as shown in Table I. All of the lines and fittings that contacted the reaction stream in the reaction system (Figure 1) were either 316 stainless steel or glass. Mass flow controllers (MKS, type 1259C) were controlled with a MKS 247C 4-channel readout.

2.3. SAMPLE EXTRACTION AND ANALYSIS

Immediately after each experiment, 10.0 mL of distilled water were added to the denuder, the denuder was capped, shaken for approximately 1 minute, and the resulting extract was poured into a cleaned high density polyethylene (HDPE) bottle

and refrigerated. The three filters in the filter pack were placed into separate 15 mL polypropylene centrifuge tubes and stored in a freezer until extraction. Filters were extracted by adding 10.0 mL of distilled water to the polypropylene tube, sonicating in the dark for 1 hour, letting the solutions sit in the dark at room temperature for 12–48 hr, removing the extracted filter and then refrigerating the extract solutions until analysis. Extract solutions of Whatman 41 filters were filtered (0.22 μm Teflon, MSI) prior to refrigeration. In some experiments the reaction flask was also extracted: a known volume of water was added to the flask, swirled around for several minutes, collected, and then refrigerated in an HDPE bottle until analysis.

Extracts were analyzed for Br^- and other anions using a Dionex DX-100 ion chromatograph with ASRS-I suppressor, TS-2 thermal stabilizer module, AG4A-SC guard column and AS4A-SC analytical column. The eluent (1.8 mM CO_3^{2-}/1.7 mM HCO_3^-) was pressurized with helium and run at a flow rate of 2.0 ml min^{-1}. The detection limit for bromide was typically 0.1 μM. Sodium concentrations were determined with a Perkin Elmer 3110 atomic absorption spectrometer with air/acetylene flame (detection limit ≈ 0.5 μM).

2.4. AEROSOL CHARACTERIZATION

The aerosol produced from the Collison nebulizer was characterized using a modified version of the aerosol reaction system in which wet particles were sent through the reaction flask and then dried with a diffusion drier prior to analysis with a differential mobility analyzer (TSI 3071) in conjunction with the TSI 3020 CNC. Under these conditions the dry particles were found to have a number median diameter of 0.026 μm and a logarithmic standard deviation of 0.72 (i.e., highly polydispersed). Diameters of deliquesced NaBr particles at a given RH were determined by interpolating NaBr data reported by Weast (1981) and Hamer and Wu (1972). At the typical RH value of 70%, the deliquesced particles were calculated to have a number median diameter of 0.046 μm, a volume mean diameter of 0.10 μm, a bromide concentration of 5.7 M, and to be 41.1% NaBr by weight. In each experiment the particles should have been deliquesced, since the experimental RH (range = 61–74%) was always above the deliquescence RH of NaBr (58%; Weast, 1981).

2.5. BROMINE CALCULATIONS

Because the goal of the denuder was to collect gas phase bromine compounds (e.g., Br_2 and HOBr), it was necessary to first characterize any interference from the collection of NaBr particles. The diffusion distance, l, that a particle can travel in time t is equal to $(2Dt)^{\frac{1}{2}}$, where D is the diffusion coefficient (Fuchs, 1964). The diffusion distance for NaBr particles in our system ranged from 0.023–0.048 mm, based on the typical residence time in the denuder ($t = 0.40$ s) and on literature values for diffusion coefficients (2.9×10^{-5} and 6.8×10^{-6} cm^2 s^{-1} for particles

with diameters of 0.05 and 0.10 μm, respectively; Fuchs, 1964). Thus, with a 1 mm annular space, approximately 5–10% (2 *l*/1 mm) of the particles that entered the denuder should have been deposited there, assuming an accommodation coefficient of 1.

In order to correct for this collection of particulate bromide on the denuder, 'blank' experiments (with the ozonator off) were run within 4 days prior to (or, in a few cases, after) every ozone experiment. Each set of blank and ozone experiments were run under nearly identical conditions (N, RH, time), except for the presence or absence of ozone. The amount of bromide collected on the denuder in the blank experiments was 9.1 $\pm$ 4.9% (mean $\pm$ 1σ; range = 2.2–18%) of the total amount of bromide collected in the denuder-filter pack. This value is consistent with that derived from the diffusion distance calculation above.

Based on this and other data (see below), we therefore assumed that all of the bromine collected on the denuder in the blank experiments was particulate bromide, Br(p). (Note that this could not be confirmed using Na^+ measurements; particulate sodium on the denuder could not be determined since Na_2CO_3 was used as the coating solution.) In experiments with ozone, the Br collected on the denuder was assumed to be a mixture of particulate and gaseous bromine. The amount of gaseous bromine collected on the denuder during a given ozone experiment, D{Br(g)}, was calculated by subtracting the amount of particulate bromide collected during the corresponding blank experiment, D{Br(p)}, from the total amount of bromine collected in the ozone experiment, D{Br(tot)}:

$$\mathrm{D\{Br(g)\}} = 1.12\left[\mathrm{D\{Br(tot)\}} - \mathrm{D\{Br(p)\}}\left(\frac{\mathrm{N_{O_3}}}{\mathrm{N_{Air}}}\right)\left(\frac{t_{\mathrm{O_3}}}{t_{\mathrm{Air}}}\right)\right]. \quad (1)$$

As shown in Equation (1), the value for D{Br(p)} from the blank experiment was normalized to conditions of the ozone experiment by multiplying it by the ratio of particle number concentrations (i.e., N in ozone experiment/N in blank experiment) and the ratio of collection times (i.e., time for ozone experiment/time for blank experiment). These corrections were small (the product of these ratios was between 0.95 and 1.15) in all except one experiment (#23, where the product was 2.09). For ozone experiments, corrected values for D{Br(p)} were, on average, 23 $\pm$ 5.3% of D{Br(tot)} (range = 14–33%). (The value from experiment #32 (46%), where N_2 was used in place of air, was not included in these statistics.). The factor of 1.12 in Equation (1) corrects for the small amount of reactor flow that went to the CNC rather than the DFP. The relative standard deviation (RSD) for D{Br(g)} was estimated to be 31–35%, primarily because of uncertainties in D{Br(p)}.

In each O_3 experiment the rate of collection of gas-phase bromine on the denuder, $R_{\mathrm{Br(g)}}$, was determined as

$$R_{\mathrm{Br(g)}} = \mathrm{D\{Br(g)\}}/t_{\mathrm{O_3}}\,. \quad (2)$$

For a given experiment, the RSD for $R_{\mathrm{Br(g)}}$ was the same as for D{Br(g)} (31–35%) since $t_{\mathrm{O_3}}$ was known quite accurately. Calculation of $k_{\mathrm{W,OX}}$, the rate constant

for oxidation of wall-deposited bromide, is described in Section 3.2.2 and the Appendix.

3. Results and Discussion

3.1. CONTROLS

Extracts of blank denuders and filters (Zefluor and KOH-impregnated Whatman 41) contained no detectable bromide. Extracts of blank Zefluor filters contained no detectable sodium. Sodium could not be measured accurately in the rinse of the reaction flask since variable background levels of Na^+ were leached from the flask.

The ability of the denuders to collect Br_2 (and HOBr) was tested by running Aadco air (2.2 slpm, T = 20 °C) through a Br_2 permeation source (Impey *et al.*, 1997), a Na_2CO_3-coated denuder, and then an alkaline bubbler containing 30 mM bicarbonate and 5 mM bisulfite to collect any residual Br_2 (or HOBr). In these tests the denuder collected 93 ± 2% of the gas-phase bromine in the air stream, independent of relative humidity (for RH = 2–82%). Because the reaction of Br_2 with Na_2CO_3 on the denuder wall likely produces HOBr (e.g., possibly through the reaction $Br_2 + Na_2CO_3 + H_2O \rightarrow HOBr + NaBr + NaHCO_3$), these tests suggest that the denuders also efficiently collected HOBr.

With two exceptions, there was no detectable bromine on the Whatman 41 filters downstream of the Zefluor filter in the dark experiments, indicating that bromide collected on the Zefluor was not volatilized. In the two exceptions (experiments 7 and 12) the amount of bromide collected on the Whatman 41 filters was roughly consistent (3.5 and 4.8 times higher, respectively) with the amount of bromide on the Zefluor filter that should have been oxidized by O_3 based on the known aqueous phase rate constant (Hoigné *et al.*, 1985). In the light experiments there was much more extensive loss of Br^- from the Zefluor filters, as will be discussed.

3.2. EXPERIMENTS IN THE DARK

3.2.1. *Dark Experiments: Initial Observations*

As shown in Table I and Figure 2, appreciable amounts of gas phase bromine were formed during experiments in which sodium bromide particles and ozone were sent to the reactor in the dark. As discussed below, the amount of Br(g) formed in these experiments was much greater than expected based on the known aqueous phase reaction of bromide with ozone, and appears to be due to reactions occurring on the walls of the reactor. A few observations are readily apparent from Table I. First, $R_{Br(g)}$, the rate of Br(g) formation, was only weakly dependent upon particle number concentration in the range of 10^4–10^7 cm^{-3}. For example, decreasing N from 10^7 (experiment 7) to 10^5 cm^{-3} (experiment 12) only decreased $R_{Br(g)}$ by a factor of ~2. A further ten-fold decrease in N to 10^4 cm^{-3} (experiments 20 and 23) only decreased $R_{Br(g)}$ by a factor of ~3. Second, as shown in Figure 2, for those

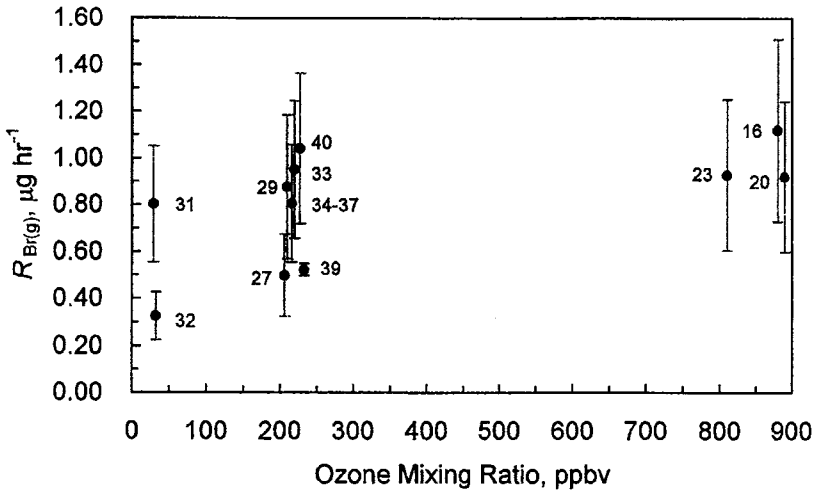

Figure 2. Rate of gas phase bromine collection ($R_{Br(g)}$ as a function of ozone mixing ratio for dark experiments with N $\approx 2 \times 10^4$ particles cm^{-3}. Each data point is labeled with the experiment number. Error bars represent $\pm$ 1 standard deviation.

experiments at the lowest particle number concentrations ($\sim 2 \times 10^4$ cm^{-3}), $R_{Br(g)}$ appears to be only weakly (and non-linearly) dependent upon the mixing ratio of ozone employed.

3.2.2. *Dark Experiments: Evidence for Wall Reactions*

To determine whether particulate bromide was being oxidized during ozone exposure in the dark, we examined the Br/Na ratios in extracts from the Zefluor filters. This ratio should be less than unity if particulate bromide was a source of Br(g). As expected, filters collected from the blank (no ozone) runs had ratios that were not significantly different from unity: 1.00 ± 0.05 (mean $\pm 1\sigma$; N = 9). However, the Br/Na ratios on filters collected during ozone experiments in the dark were also not significantly different from unity (1.04 ± 0.06; N = 9; experiments with $\sim 2 \times 10^4$ particles cm^{-3}), indicating that the NaBr particles were not a significant source of the observed Br(g). This result suggests that bromide deposited to the flask walls, Br(w), was the precursor for the gas phase bromine produced.

In order to test this hypothesis, concentrations of bromide in the reaction flask were measured following four experiments under nearly identical conditions of exposure time and particle concentration. As shown in Table II, at the end of the blank experiment (#30) there were 48 nmol of Br on the walls of the flask and (by definition) no Br(g) on the denuder. In the presence of O_3 (29 ppbv; experiment 31) there were 20 nmol of Br on the walls of the flask and 30 nmol of Br(g) collected on the denuder at the end of the experiment. The amount of Br(w) 'missing'

Table II. Mole balance of bromine in reaction system

Expt. no.	O_3 ppbv	Nanomoles of Br or Na[a]					Nanomoles of NO_3^- in reactor[b]
		Denuder	Reactor	Teflon filter		Total	
		D{Br(g)}	Br(w)	Br(p)	Na(p)	Br	
30	0	0[c]	48	76	74	124	16
31	29	30	20	91	86	141	13
32[d]	32	12	42	103	97	157	8.8
33	220	36	26	96	91	158	9.4

For each experiment N = (1.8–2.0) × 10^4 cm^{-3} and reaction time = 180 min. Values for the denuders and Teflon filters are corrected for the fraction of reaction flask flow sent to the CNC.

[a] Amount of bromine or sodium on component at end of given experiment. Sodium concentrations in the denuder could not be reliably determined because of very high background levels of Na from the Na_2CO_3 used to coat the denuders. Sodium in the flask could not be reliably measured because leaching of Na from the glass surfaces during extraction led to large and variable blank concentrations. Relative standard deviations were approximately ±30% for D{Br(g)} and ±5% for the other quantities.

[b] Amount of nitrate in reactor at end of experiment. Concentrations of nitrate in the denuder, and concentrations of nitrite in the reactor and denuder, were all below detection limits. Concentrations of nitrate and nitrite on the Teflon filter could not be reliably determined because of variable background concentrations.

[c] There were 9.2 nmol of Br, assumed to be from particulate bromide, collected on the denuder in experiment 30. The amounts of D{Br(p)} on the denuders in experiments 31–33 were assumed to be the same.

[d] Aadco air replaced with N_2 from cylinder (see Table I).

from the walls of the reaction flask in this experiment was approximately 35 nmol (calculated as (48 × 141/124) − 20; where the 141/124 factor is the ratio of total DFP Br in the ozone and air experiments, used to approximately scale values for different amounts of bromide loading in the flask; Table II). Thus the amount of D{Br(g)} collected in this ozone experiment (30 nmol) was approximately equal to the amount of Br(w) 'missing' from the walls of the reaction flask (35 nmol).

The results from experiments 32 and 33 (Table II) are similar to those described above for experiment 31. In these experiments the values for D{Br(g)} were within 40% (experiment 32) and 3% (experiment 33) of the scaled amount of wall-deposited bromide that appeared to have been removed during O_3 exposure. (These differences were likely a result of differences in denuder collection of Br(p) between experiments.) In addition, for all three ozone experiments (31–33) there was no bromide missing from the Teflon filter (i.e., Br(p)/Na(p) $\geqslant$ 1 on the filters; Table II), indicating there was no significant loss of Br from the particles. (This same ratio could not be determined in the reaction flask because of leaching of sodium from the glass.) Together, these observations reveal that wall-deposited Br was the source of gas-phase bromine.

To quantitatively interpret these results, we have constructed a kinetic model that describes the reactions of particulate, wall-deposited, and gaseous bromide (Br(p), Br(w), and Br(g), respectively). As shown in the Appendix, this model predicts that, under conditions where the oxidation of particulate bromide is an insignificant source of gaseous bromine, the total amount of Br(g) collected on the denuder by time t is

$$\mathrm{D\{Br(g)\}} = R_{\mathrm{Br(w)}}t + \left(\mathrm{Br(w,0)} - \frac{R_{\mathrm{Br(w)}}}{k_{\mathrm{W,OX}}}\right)(1 - \mathrm{e}^{-k_{\mathrm{W,OX}}t}), \qquad \text{(A6)}$$

where $R_{\mathrm{Br(w)}}$ is the rate of deposition of Br(p) to the flask walls, Br(w,0) is the amount of bromide present on the flask walls at the beginning of ozone exposure, and $k_{\mathrm{W,OX}}$ is the apparent first-order rate constant for oxidation of bromide deposited to the flask walls. As discussed previously (Section 2.2), we define time zero as the moment when the flow of particles and ozone from the reaction flask is first sent to the denuder/filter pack. The determination of $R_{\mathrm{Br(w)}}$ and Br(w,0) are described in the Appendix. Values of $k_{\mathrm{W,OX}}$ were determined by solving Equation (A6) with the experimental data (D{Br(g)}/2 at time t) using the 'Curve Fit' routine of SigmaPlot (Version 1.02). We used half of the measured amount of gaseous bromine on the denuder (i.e., D{Br(g)}/2) because we assumed that the initial rate-limiting oxidation of Br^- (the process of interest) produced a mono-bromine species (e.g., HOBr) that was then quickly converted to Br_2 by subsequent reactions (e.g., via R3). That is, we have assumed that the amount of gaseous bromine collected on the denuder is twice the amount initially produced by the reaction of interest involving ozone. We have made this assumption because work by DeHann *et al.* (1999) has shown that the oxidation of particulate NaBr(aq) by ozone releases Br_2(g), but oxidation of Br^- by O_3 or $^{\cdot}OH$ will initially produce a mono-bromine product (e.g., R1 or R11). However, if HOBr(g) or some other mono-bromine species was the dominant gaseous bromine product collected in our experiments, or if Br_2 was formed from the initial reaction step and not as a result of subsequent steps, then our values of $k_{\mathrm{W,OX}}$ will be underestimated by up to a factor of ~ 2.

Besides this potential underestimation, the greatest uncertainty in calculating $k_{\mathrm{W,OX}}$ resulted from uncertainty in values of D{Br(g)}/2. Therefore, to estimate the standard deviation for $k_{\mathrm{W,OX}}$ in a given experiment, we solved Equation (A6) using [D{Br(g)}/2 + 1σ] and [D{Br(g)}/2 − 1σ] to determine values of $k_{\mathrm{W,OX}} + 1\sigma$ and $k_{\mathrm{W,OX}} - 1\sigma$, respectively. For experiments 16, 20, and 23 there was another significant source of uncertainty, namely error in the estimated value of $R_{\mathrm{Br(w)}}$ (this quantity was measured in other experiments). For these three experiments, we first calculated standard deviations in $k_{\mathrm{W,OX}}$ due to uncertainty in D{Br(g)}/2 as described above, and then repeated the process (with the best estimate of D{Br(g)}/2) by using values of $R_{\mathrm{Br(w)}} \pm 1\sigma$ in (A6). The total RSD's in these three experiments were then estimated by combining the relative standard deviations in $k_{\mathrm{W,OX}}$ due to

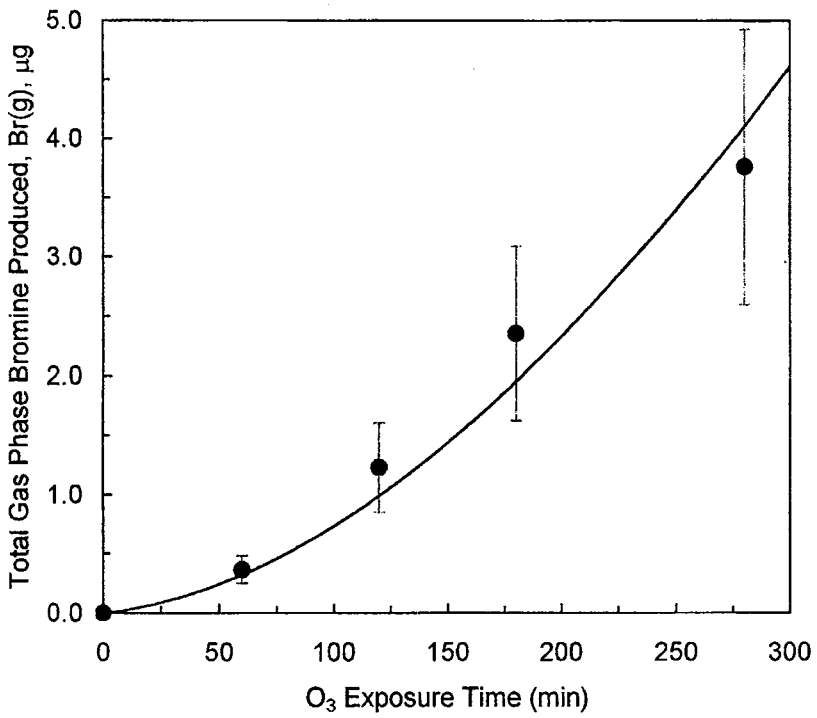

Figure 3. Time dependence of gas phase bromine formation. Data points (circles, with ± 1 standard deviation error bars) are from experiments 34–37 (220 ppbv O_3, N = 2.0×10^4 cm^{-3}). The solid line is a fit of Equation (A6) to the experimental data; the calculated value for $k_{W,OX}$ from this fit is 0.15 hr^{-1}.

D{Br(g)} and $R_{Br(w)}$. (This combination was done by taking the square root of the sum of the squares of the two RSD values.)

The fit of Equation (A6) to the experimental data from experiments 34–37 (the only series containing more than two data points) is shown in Figure 3. The good fit in this figure suggests that the derived equation has the appropriate functional form. The fact that the rate of Br(g) collection (i.e., the slope of the line in Figure 3) increases with increasing time indicates that, in a given experiment, apparent values of $R_{Br(g)}$ (Table I) depend upon the time of ozone exposure. In addition, the dependence of D{Br(g)} on Br(w,0) (Equation A6), indicates that values for $R_{Br(g)}$ also depend upon the amount of time that the flask was pre-loaded with Br^- prior to O_3 exposure.

Calculated values for $k_{W,OX}$ are listed in Table I and plotted versus ozone mixing ratio in Figure 4. These data reveal that the rate constant for oxidation of wall-deposited bromide was apparently independent of ozone mixing ratio. Although it appears that $k_{W,OX}$ was somewhat lower at the highest ozone mixing ratios tested

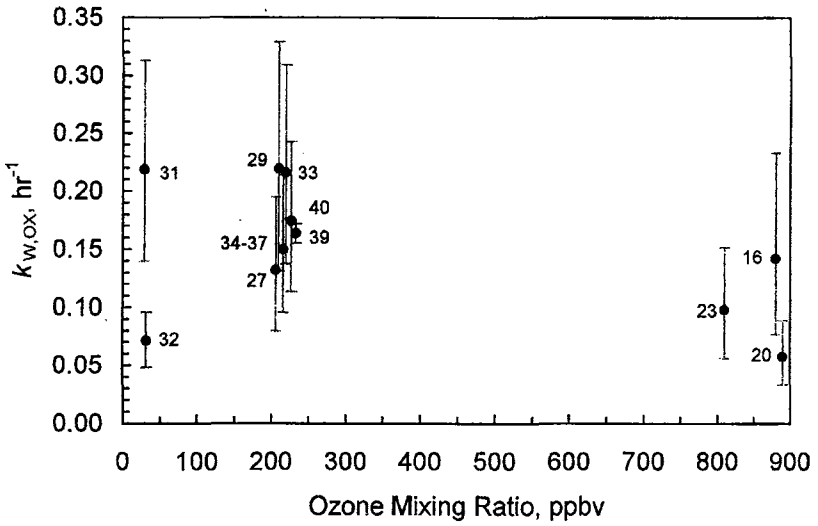

Figure 4. Apparent first-order rate constant for oxidation of wall-deposited bromide $k_{W,OX}$), as a function of ozone mixing ratio, for experiments with N $\approx 2 \times 10^4$ cm^{-3}. Each data point is labeled with the experiment number. Rate constants in experiments 16, 20, and 23 were calculated using the average value for $R_{Br(w)}$ from the other experiments (see Table I). Error bars represent $\pm$ 1 standard deviation.

(experiments 16, 20, and 23), this could be due to factors which would lead to underestimation of $k_{W,OX}$. For example, this would have happened if actual values of $R_{Br(w)}$ in these experiments were lower than the average value (which was used to calculate $k_{W,OX}$ for these experiments). As for the dependence of reactivity on the amount of bromide, the estimated value of $k_{W,OX}$ for the one experiment (#7) at higher N (2×10^7 cm^{-3}) was approximately 10 times lower than the values obtained at N $\approx 10^4$ cm^{-3}. While this one estimated result is consistent with the dependence of $R_{Br(g)}$ on N discussed previously (i.e., a weak, non-linear dependence on N; Section 3.2.1), it is not consistent with our kinetic model assumption that $k_{W,OX}$ should be independent of the amount of Br(w).

Other properties of the observed reactivity are also apparent from the $k_{W,OX}$ data of Table I and Figure 4. First, the formation rate of gaseous bromine appears to depend upon the presence of molecular oxygen in the system, as indicated by comparing experiment 31 (29 ppbv O_3, 21.6% oxygen; $k_{W,OX} = 0.22$ hr^{-1}) with experiment 32 where Aadco air was replaced with high purity N_2 (32 ppbv O_3, 0.83% O_2; $k_{W,OX} = 0.071$ hr^{-1}). Second, substituting cylinder zero air for the Aadco-treated air made no significant difference in Br(w) oxidation rate constants (compare experiment 29 with 33), suggesting that trace constituents in the Aadco air were not responsible for the observed oxidation of bromide.

In addition, although values for $k_{W,OX}$ were relatively independent of the ozone mixing ratio (Figure 4), it does appear that bromide oxidation in this system required ozone. This is suggested by the previously discussed observations that the amount of Br collected on the denuder during blank experiments (i.e., no ozone) was consistent with uptake of particulate bromide, while the amount collected during ozone exposure was much higher. On average, the amount of Br(g) collected during the ozone experiments was 3.3 times higher than the amount of Br(p) collected during the corresponding blank experiments.

We carried out two additional experiments to test our conclusions that the denuder was primarily collecting Br(p) in the blank experiments, and that wall-deposited bromide was the source of gas phase Br. In the first experiment (#39), the reactor was pre-loaded with NaBr particles for approximately 2 hours (in the absence of ozone), the particle flow was stopped, and then the flask was exposed to ozone (without additional particles). Thus, in this case, only Br(w) was available for oxidation and there was no collection of Br(p) on the denuder. In a second experiment (#40), the flask was pre-loaded for ~ 2 hours (in the absence of ozone) and then ozone exposure was started with the particle flow continuing. (Note that this latter experiment is similar to experiments 27 through 37, except with a much longer pre-loading time.) In both of these experiments, the resulting values of $k_{W,OX}$ (0.16 and 0.18 hr^{-1}, respectively; Table I) were in the same range as for the earlier experiments (#27, 29, 31, 33, 34–37) confirming that: (i) the correction for Br(p) collected on the denuder was valid; (ii) wall-deposited bromide was the source for the oxidized bromine species; (iii) the particulate bromide was, at most, a minor source of Br(g) in our experiments, and (iv) our kinetic model adequately described the reaction system, at least for $N \approx 10^4$ cm^{-3}. Finally, it is interesting to note that for experiment #39 D{Br(g)} could be determined directly (i.e., without a correction for D{Br(p)}; see Equation (1)), and therefore the uncertainties for $R_{Br(g)}$ and $k_{W,OX}$ in this experiment were much lower than in other experiments.

As mentioned above, we have calculated values for $k_{W,OX}$ assuming that there was a negligible contribution to Br(g) from the oxidation of particulate bromide. If we instead assume that particulate bromide was oxidized with the same rate constant as wall-deposited bromide (i.e., $k_{P,OX} = k_{W,OX}$; see Appendix) then, with a residence time of only ~ 2 minutes, at most only a few percent of Br(p) would have been oxidized. As this amount is too small to be detected using Br/Na ratios, we cannot rule out the possibility that particulate bromide was oxidized at the same rate as the wall-deposited bromide. However, if Br(p) was as reactive as Br(w), this would have caused only minor decreases in reported values of $k_{W,OX}$ (Table I), which were calculated assuming Br(p) was not oxidized. For example, for experiments 34–37, assuming $k_{P,OX} = k_{W,OX}$ (see Equation (A5)) decreases $k_{W,OX}$ by only 7.5%. This potential oxidation of Br(p) has only a minor effect because, over the course of an experiment, Br(w) was typically much greater than Br(p). For example, Br(w) was typically 20–30 times greater than Br(p) at the half-way point of the experiments.

3.2.3. *Dark Experiments: Possible Mechanisms for Bromide Oxidation*

While bromide can be oxidized by certain NO_y species (De Haan *et al.*, 1999), and low concentrations of NO_y were measured in our reaction system (Table I), available evidence suggests that NO_y species were not the primary oxidant of Br(w). Oxidation of wall-deposited bromide by NO_y should form Br(g) (which would be collected on the denuder) and nitrate (which would be left in the flask). However, the average rate of nitrate collection in the flask in the blank (no ozone) experiments (3.8 ± 1.5 nmol hr^{-1}; N = 3) was essentially the same as the average in the ozone experiments (3.3 ± 0.82 nmol hr^{-1}; N = 8), despite the fact that gaseous bromine was apparently only formed in the ozone experiments. This suggests that there is a fairly steady background level of NO_y species in the system (possibly HNO_3 displaced by water vapor) that does not result in bromide oxidation. Furthermore, if NO_y species were the dominant oxidant of bromide in the reaction flask, the molar amount of nitrate in the reaction flask at the end of an experiment should have been equal to the amount of D{Br(g)} collected. However, in seven of the eight ozone experiments, the amount of D{Br(g)} collected was greater (by an average factor of 2.7) than the amount of NO_3^- in the reaction flask. If nitrate amounts in the ozone experiments are reduced by the smallest NO_3^- values from the blank experiments, the average ratio of D{Br(g)} to NO_3^- in the flask increases to 13. These points are illustrated for four specific experiments in Table II. Based on this information, it appears that NO_y species were not stoichiometrically capable of accounting for the observed bromide oxidation, but a reaction mechanism involving initiation by NO_y followed by a separate propagation cycle cannot be ruled out.

Based on the observations described above, it appears that ozone was responsible for the oxidation of wall-deposited bromide in the reaction flask. Assuming Henry's law equilibrium for ozone in our system, it is possible to calculate the expected first-order rate constant for oxidation of aqueous bromide by ozone (k'_{O_3}) using

$$k'_{O_3} = K_{H,O_3} \times p_{O_3} \times k_{O_3+Br}\,, \tag{3}$$

where K_{H,O_3} is the Henry's law coefficient for ozone (calculated for the temperature of each experiment using an enthalpy of dissolution of –5.04 kcal mol^{-1}, and K_{H,O_3} at 298 K of 0.0113 M atm^{-1}; Seinfeld and Pandis, 1998); p_{O_3} is the partial pressure of ozone in the reaction system (atm); and k_{O_3+Br} is the rate constant for aqueous oxidation of bromide by ozone (160 M^{-1} s^{-1}; Hoigné *et al.*, 1985).

As shown in the final column of Table I, the measured values of $k_{W,OX}$ for the N $\approx 2 \times 10^4$ cm^{-3} experiments were typically ~ 100 times greater than the calculated values for k'_{O_3}. That is, the apparent ozone reactivity of wall-deposited bromide in the system was typically a hundred times greater than that expected for bromide in aqueous solution. Because values of $k_{W,OX}$ were relatively independent of ozone mixing ratio, the ratio $k_{W,OX}/k'_{O_3}$ increased with decreasing ozone, exceeding 1000 for the lowest O_3 mixing ratio tested (29 ppbv in experiment #31; Table I). These results, coupled with the fact that bromide oxidation in the system

appeared to require ozone, indicate that the oxidation of deposited bromide in our system was not proceeding through the bulk aqueous phase reaction with ozone. It should be noted that this enhanced reactivity is not due to the catalytic cycle of bromine release that is thought to occur in the marine boundary layer (i.e., photolysis of Br_2 followed by R6, R7, and R3). Because the reaction flask was kept dark during our experiments there was no chance for Br_2 to undergo photolysis and lead to further bromine release from the particles via this catalytic cycle.

While our results suggest that ozone played an important role in the oxidation of wall-deposited bromide, the mechanism is unknown. In the remaining portion of this section we propose some possible pathways that might have accounted for at least a portion of the enhancement in bromide oxidation in our system. While we were unable to devise a mechanism that quantitatively explained the observed reactivity, these pathways present a qualitative picture of possible mechanisms, mostly via reactions that involve the glass surface of the reaction flask. However, it should be kept in mind that even though Br(w) was the source of the gaseous bromine, the glass surface might not have participated in the reactions that oxidized the wall-deposited bromide.

That being said, one possible reason for the increased reactivity is that the surface of the reaction flask might have directly enhanced the rate of bromide oxidation by ozone relative to the rate in bulk aqueous phase (R1–R2). Another possibility is that the glass surface converted ozone into stronger oxidants that reacted more rapidly with bromide. In aqueous solution, ozone can decompose to yield oxyradicals, such as the strongly oxidizing hydroxyl radical ($^{\bullet}OH$), via mechanisms that include (Ross *et al.*, 1998)

$$O_3(aq) + OH^- \rightarrow O_2(aq) + HO_2^- \quad \text{(R8)}$$

$$HO_2^- + H^+ \rightarrow HOOH(aq) \quad \text{(R9)}$$

$$O_3(aq) + HOOH(aq) \rightarrow {}^{\bullet}OH(aq) + HO_2^{\bullet}(aq) + O_2(aq)\,. \quad \text{(R10)}$$

Once formed, hydroxyl radical could then oxidize aqueous bromide to form dibromide radical anion (Mamou *et al.*, 1977)

$$^{\bullet}OH + Br^- \rightarrow OH^- + Br^{\bullet} \quad \text{(R11)}$$

$$Br^{\bullet} + Br^- \rightarrow {}^{\bullet}Br_2^- \quad \text{(R12)}$$

which can react with $HO_2^{\bullet}$ to form molecular bromine (Mozurkewich, 1995):

$$^{\bullet}Br_2^- + HO_2^{\bullet} \rightarrow Br_2 + HO_2^-\,. \quad \text{(R13)}$$

It is possible that the glass surface enhanced the conversion of ozone to hydroxyl radical or other oxidants, as suggested previously (Heikes *et al.*, 1982; Heikes, 1984). Heikes (1984) found that bubbling ozone through water in glass

impingers destroyed ozone, and formed hydrogen peroxide, at rates much faster than expected based on known aqueous phase chemistry. The mechanism for this reaction appeared to involve reaction of ozone at the surface of the glass walls of the impingers to form intermediates such as $^{\bullet}OH$ or $^{\bullet}O_2^-$. The loss of O_3 and formation of HOOH in these experiments slowed during exposure, eventually stopping, implying that the number of glass surface reaction sites limited the reaction rate and that the sites were eventually passivated (Heikes, 1984). In our experiments, the weak dependence of Br(g) formation on ozone mixing ratio suggests that bromide oxidation in our experiments might also have been limited by the number of available reaction sites at the glass walls. However, unlike Heikes (1984), we did not observe a decrease in reactivity with reaction time (Figure 3). In part this is because the amount of bromide in the reaction flask increased during the reaction, but it also suggests that the reactive sites on the flask were not passivated during bromide oxidation. Finally, the dependence of $k_{W,OX}$ on oxygen concentration in our system (Table I) might be an indication that the conversion of O_3 to stronger oxidants required the participation of O_2.

The rate of bromide oxidation could also be enhanced if $^{\bullet}Br_2^-$ was oxidized in a pseudo-catalytic cycle involving some trace species X. In this scheme, X oxidizes $^{\bullet}Br_2^-$ to yield Br_2 and the reduced form of X (red-X) that, in turn, forms a species capable of oxidizing bromide:

$$^{\bullet}Br_2^- + X \rightarrow Br_2 + \text{red-X} \tag{R14}$$

$$\text{red-X} + Br^- \rightarrow Br^{\bullet} + Y\,. \tag{R15}$$

One possible candidate for X is ozone, which might react via

$$^{\bullet}Br_2^- + O_3 \rightarrow Br_2 + O_3^- \tag{R16}$$

$$O_3^- + H^+ \rightarrow {}^{\bullet}OH + O_2 \tag{R17}$$

followed by Reaction (R11). Another possible identity for X is ferric iron (either at the glass surface or in solution), which might participate via the sequence

$$^{\bullet}Br_2^- + \text{Fe(III)} \rightarrow Br_2 + \text{Fe(II)} \tag{R18}$$

$$\text{Fe(II)} + H^+ + O_3 \rightarrow \text{Fe(III)} + {}^{\bullet}OH + {}^{\bullet}O_2^-\,. \tag{R19}$$

While Reactions (R17) and (R19) are known (Ross *et al.*, 1998), we were unable to find references for Reactions (R16) and (R18). However, based on reduction potentials for the relevant half-reactions (Wardman, 1989; Lide, 1999), both of these latter reactions should be spontaneous at room temperature.

Table III. Ozone exposure experiments with 254 nm illumination (T = 30–31 °C) [a]

Expt. #	Room lights	N (cm^{-3})	O_3 (ppbv) [b] Before PM and hν	O_3 (ppbv) [b] With PM and hν	Pre-load Time (min)	Denuder Time (min)	$R_{Br(w)}$ [c] ($\mu g\ hr^{-1}$)	D{Br(p)} (μg)	D{Br(g)} (μg)	$R_{Br(g)}$ ($\mu g\ hr^{-1}$)	$k_{W,OX}$ (hr^{-1})	$\frac{k_{W,OX}}{k'_{O_3}}$
8	on	2×10^7	1240	970	3	300	[48] [c]	29	92	18	[0.087]	[14]
9	on	2×10^7	1070	810	60	63	[48] [c]	6.2	15	14	[0.10]	[21]
10 [d]	on	2×10^7	940	810	21	60	[48] [c]	5.9	5.7	5.7	[0.072]	[15]
13	off	1.5×10^5	950	850	395 [e]	120	–	2.0	13	6.7	–	–
17 [f]	off	1.5×10^4	840	830	14	180	1.1	0.63 [g]	5.6	1.9	$\geqslant 12$ [h]	$\geqslant 2500$

[a] See Table I for descriptions of columns not described here. Mixing ratios of NO_y, estimated based upon later measurements, were approximately 1 ppbv for experiments 8–10 and 13. NO_y in experiment #17 was apparently much greater than this; see note f. Approximate relative standard deviations are estimated to be ± 35% for D{Br(g)} and $R_{Br(g)}$ and ± 50% for $k_{W,OX}$. Values in square brackets were either estimated (based on values in similar experiments) or calculated using at least one estimated quantity.

[b] Mixing ratio of O_3 in reaction flask prior to, and after, introduction of NaBr particles and light.

[c] Rate of deposition of NaBr particles onto walls of flask. Values for experiments 8–10 were not measured and were assumed to be equal to the measured value in the corresponding blank experiment.

[d] Nebulizer solution contained 0.100% NaBr, 0.200 M acetate, and was adjusted to pH 3.9.

[e] 950 ppbv ozone had flowed through system for 225 min of this.

[f] Aadco air generator was malfunctioning during this experiment; see text.

[g] Assumed that particles collected on denuder had same Br deficiency as those collected on Teflon filter (Br/Na = 0.54).

[h] Value of $k_{W,OX}$ is lower bound because essentially no Br(w) was found at end of experiment (1.5 nmol). $k_{P,OX} = 16\ hr^{-1}$ for this experiment.

3.3. EXPERIMENTS WITH 254 NM RADIATION

3.3.1. *Light Experiments: Initial Observations*

As listed in Table III, in five experiments the reaction flask was exposed to a combination of ozone and 254 nm illumination (and, in three of these cases, to room light). Based on measured Br/Na molar ratios (0.99–1.05) in the filter packs of these experiments, it appears that particulate bromide was not significantly oxidized, with the exception of experiment #17 (Br/Na = 0.54) which is discussed below. These observations indicate that Br(w) was also the source of gaseous bromine collected on the denuder in the light experiments.

Based on a comparison of experiments 8 and 13 with the corresponding dark experiments (7 and 12, respectively), it appears that the rate of production of gaseous bromine was approximately 2–3 times greater in the presence of 254 nm radiation (Table III). Similarly, based on the first three light experiments (#8–10; N = 2×10^7 cm^{-3}), calculated values of $k_{W,OX}$ were approximately 4–6 times greater than those in the corresponding ozone experiment in the dark (#7; Table I), and were 14–21 times greater than expected from the aqueous phase reaction of ozone with bromide. However, it should be noted that these latter observations are tentative since they are based on only one dark experiment.

As shown in Table III, for all light experiments (except #17) the mixing ratio of O_3 decreased by 11–24% in the presence of particles and light. This decrease in O_3 was not observed with 254 nm light in the absence of NaBr particles (i.e., it was not due to direct photolysis of O_3), nor was it observed in dark experiments with particles. These observations suggest that the loss of O_3 in the light experiments was the result of $Br^{\bullet}$-catalyzed destruction.

3.3.2. *Light Experiments: Possible Mechanisms for Bromide Oxidation*

The apparently greater values of $k_{W,OX}$ in the light experiments, compared to that in the corresponding dark experiment, suggest that the presence of UV-radiation yielded higher concentrations of oxidants such as $^{\bullet}OH$, or formed additional oxidants. In the presence of 254 nm radiation, formation of hydroxyl radical would occur from the direct photolysis of gas phase ozone (and subsequent reaction of $O(^1D)$ with water vapor) as well as from the sequence (Mozurkewich, 1995)

$$O_3(g) + {}^{\bullet}OH(g) \rightarrow HO_2^{\bullet}(g) + O_2(g) \tag{R20}$$

$$HO_2^{\bullet}(g) \rightarrow HO_2^{\bullet}(aq) \tag{R21}$$

$$HO_2^{\bullet}(aq) \rightarrow {}^{\bullet}O_2^- + H^+ \tag{R22}$$

$${}^{\bullet}O_2^- + O_3(aq) + H^+ \rightarrow {}^{\bullet}OH(aq) + 2\,O_2(aq)\,. \tag{R23}$$

Additional evidence for the presence of higher total concentrations of oxidants in the light experiments comes from the fact that there were significant losses of Br from the Zefluor filters (as evidenced by collection of Br on the downstream W-41 filters) that were not seen in the dark experiments. The amounts of bromide lost from the Zefluor filter were approximately 10–50 times greater than expected based solely on ozone oxidation.

To see whether the observed bromine collection and O_3 loss in the light experiments could be predicted by known chemistry, we constructed a simple heterogeneous model (32 species, 130 reactions and mass transfer steps) using Acuchem (Braun *et al.*, 1988). The model (not shown) was based on the conditions of experiment #9 and consisted of an aqueous phase, to represent liquid on the flask walls, and a gas phase. Because of the limitations of Acuchem, the amount of liquid water present on the flask walls had to be constant, and was set equal to the estimated total amount collected by the end of the experiment (2.1×10^{-7} L). The initial aqueous bromide concentration was set equal to 5.7 M, that expected in deliquesced NaBr at 70% RH, and ozone was assumed to be in Henry's law equilibrium. In the model we used the literature rate constant for the reaction between ozone and bromide (160 M^{-1} s^{-1}; Hoigné *et al.*, 1985), rather than the calculated value from our dark experiment. However, at the particle number concentration of the modeled 254 nm irradiation experiments (2×10^7 cm^{-3}), the calculated rate constant was only 2.4 times higher than the literature value (i.e., $k_{W,OX}/k'_{O_3} = 2.4$ for experiment #7; Table I). (Recall from Section 3.2.1 that $R_{Br(g)}$ was only weakly dependent upon N; hence $k_{W,OX}$ will decrease with increasing N.)

We found that the model could reproduce the measured amount of Br(g) collected on the denuder in experiment #9, as well as the observed loss of $O_3(g)$, only if two assumptions were made: (i) there was a source of protons to the aqueous phase of approximately 2×10^{-4} mol L^{-1} s^{-1}, and (ii) the rate constant for $Br_2(g)$ photolysis (j_{Br_2}) was 0.1 s^{-1}. With these assumptions, the pH of the aqueous phase

generally stayed between 5.6 and 6.0, the model exhibited a catalytic cycle of Br^- oxidation and O_3 destruction (i.e., R3, R6, R7), and the modeled value of D{Br(g)} matched the experimental value. In the absence of the proton source, the pH of the aqueous phase rose to pH $\sim$ 8 by the end of the model run, and the amount of Br(g) produced was approximately consistent with that expected from the oxidation of Br^- by ozone (and subsequent volatilization of HOBr), i.e., much less than observed experimentally. There was no loss of O_3(g) in this case. If the model contained a proton source, but a smaller value of j_{Br_2}, the amount of Br(g) produced was comparable to that measured experimentally, but there was very little loss of O_3(g).

The assumed proton source and value for j_{Br_2} are both very high and seem out of the range of possibility for our system. For example, taking into account the major and minor emission lines of the Hg lamp used in the experiment, we estimate that j_{Br_2} should have been 5×10^{-6} s^{-1}. This suggests that the model did not entirely capture the chemistry that occurred during our experiments. Based on the results from the dark experiments, it seems likely that some portion of the observed reactivity in the experiments with 254-nm radiation was also due to interactions of ozone with the walls of the glass reaction flask.

A few past studies have found that glass and other surfaces can enhance the oxidation of halides in the presence of light. For example, borosilicate glass walls (Duran 50, Schott) were found to catalyze the oxidation of chloride in the presence of ozone and light ($\lambda > 360$ nm), while no reaction was observed in Teflon bags unless quartz aerosol (Aerosil 200, Degussa) was added (Behnke and Zetzsch, 1989; Behnke *et al.*, 1995). The authors proposed that these oxidations involved the conversion of ozone to hydroxyl radical at the glass or quartz surfaces. Chloride oxidation was also observed in illuminated Teflon bags containing O_3, HCl, and either TiO_2, SiO_2, or Fe_2O_3 aerosols (Behnke and Zetzsch, 1990; Behnke *et al.*, 1995). In these experiments, chloride oxidation was suggested to proceed through photo-oxidation of chloride at the aerosol surface.

3.3.3. *Light Experiments: Evidence for Bromide Oxidation by NO_y Species in Experiment #17*

As noted above, there was one light experiment (#17) which yielded results very different from the others. At the end of this experiment it was discovered that the Aadco air generator had malfunctioned, and the air used in the experiment appeared to have been significantly contaminated with NO_x and hydrocarbons (as evidenced by large amounts of nitrate and organic acids in the reaction flask after the experiment). Unlike every other light and dark experiment, this was the only experiment where particulate bromide (Br(p)) was noticeably oxidized, as evidenced by a Br/Na ratio on the Teflon filter of 0.54. Based on the residence time of the reactor and the amount of Br(p) lost from the particles, the calculated value for $k_{P,OX}$, the pseudo-first order rate constant for oxidation of Br(p), was 16 hr^{-1}. Bromide on the flask walls was also rapidly oxidized in this experiment, with a

calculated lower bound for $k_{W,OX}$ of 12 hr^{-1} (Table III). These two rate constants are roughly 3000 times greater than the value expected based on O_3 oxidation. Furthermore, the fact that they're comparable suggests that the same oxidation mechanism was responsible in both cases.

Unlike the dark experiments described earlier, in experiment 17 the number of moles of NO_3^- in the reaction flask was greater (by a factor of 3.2) than the number of moles of Br(w) oxidized. Similarly, the number of moles of NO_3^- on the Teflon filter was 1.7 times greater than the number of moles of Br^- lost from the filter in this experiment. Thus some NO_y species could have been responsible for the observed rapid oxidation of both the particulate and the wall-deposited bromide in experiment 17. Possible oxidants include $NO_3^{\bullet}$ and N_2O_5, both of which rapidly oxidize bromide (Ross *et al.*, 1998; Finlayson-Pitts *et al.*, 1990).

3.4. POSSIBLE ENVIRONMENTAL IMPLICATIONS

Our results suggest that the ozone oxidation of bromide on a borosilicate glass surface proceeds much more rapidly than the same reaction in bulk aqueous solution. As discussed above, there are also a few reports of glass, quartz, or metal oxide surfaces enhancing the oxidation of chloride in the presence of ozone and light (Behnke and Zetzsch, 1989, 1990; Behnke *et al.*, 1995), and of glass surfaces enhancing the aqueous conversion of ozone to other oxidant species (Heikes *et al.*, 1982; Heikes, 1984). It is interesting to note that Heikes (1984) found that the aqueous conversion of O_3 to HOOH on Teflon surfaces was even more rapid than on borosilicate glass. In addition, several other studies have shown that ozone reacts with a number of other surface types more relevant to atmospheric chemistry. For example, Jans and Joigné (2000) reported that carbon black catalyzed the conversion of ozone to hydroxyl radical in aqueous solution. Similarly, ozone reacts with a number of different types of suspended particles in air, including soot (Kamm *et al.*, 1999, and references therein), SiO_2, TiO_2, coal fly ash, and wood ash (Alebic-Juretic *et al.*, 1997). Ozone can also be destroyed by sand and soil surfaces, presumably via reactive uptake (as summarized by Dentener *et al.*, 1996). Taken together, these observations suggest that ozone reacts with a wide variety of atmospheric particles, and that at least a portion of the reacted O_3 can be converted to other oxidants such as $^{\bullet}OH$.

A recent model study has predicted that mineral aerosol can lead to reductions in tropospheric ozone mixing ratios, primarily through direct reaction at the particle surface, and that this effect might occur to a small but significant extent over oceanic regions downwind of dust sources (Dentener *et al.*, 1996). Mineral dust is the most abundant atmospheric particle type by mass (Seinfeld and Pandis, 1998) and is widespread over the oceans as a result of long-distance transport from source regions such as Asia and Africa (e.g., Dentener *et al.*, 1996). In addition, sea salt particles are often internally mixed with silicate dust particles (Andreae *et al.*, 1986; Niimura *et al.*, 1994; Jacobson, 2001), apparently as a result of cloud-

processing (Andreae *et al.*, 1986). In combination with our results, these field and modeling results suggest that reaction with ozone in mixed sea-salt/silicate particles might be a significant mechanism for halide oxidation in the MBL. Of course there are a number of important uncertainties in this suggestion, including morphological and compositional differences between borosilicate glass and mineral aerosols (though both are primarily SiO_2), and the mechanism of halide oxidation.

In addition to soil dust, inclusion of other particle types into sea-salt particles might also lead to significant changes in their chemistry. For example, a recent modeling study by Jacobson (2001) indicated that a portion of black carbon particles become internally mixed with sea-salt particles over the period of a few days. In conjunction with the results of Jans and Joigné (2000), which showed that carbon black can convert ozone to hydroxyl radical in aqueous solution, this suggests that the presence of black carbon might affect the chemistry of halides, as well as S(IV) and organic carbon, in sea-salt particles.

4. Conclusions

In the presence of ozone, bromide deposited to the walls of a borosilicate glass flask was oxidized in the dark to yield gaseous bromine species, Br(g). Based on measured concentrations of nitrate in the reaction flask, NO_y species were not responsible for this oxidation. Rather, it appeared that ozone initiated the oxidation of bromide, although the rate of Br(g) formation was relatively independent of O_3 mixing ratio in the range of 30–1000 ppbv. The rate of Br^- oxidation in these dark experiments was faster than expected (from the known aqueous phase reaction with O_3) by factors ranging from ~ 100 to ~ 1000. While the reactions responsible for the observed chemistry are unknown, they appear to involve ozone and the glass surface of the reaction flask, possibly via the formation of reactive intermediates such as hydroxyl radical. Several previous studies have also found that glass surfaces can significantly increase the rates of reactions, although the mechanisms were not determined in these cases either.

We have also found that the ozone-initiated rate of bromide oxidation apparently increased in the presence of 254 nm radiation. In these cases, there was a decrease in O_3 mixing ratio that was consistent with that expected from Br-radical chemistry. As in the dark, the mechanisms responsible for the oxidation of wall-deposited bromide in the presence of light were unknown.

The environmental implications of a possible enhancement in halide oxidation by ozone at the surfaces of silicate and other particles are unclear but might be significant, especially since silicate and sea-salt particles are often internally mixed in the MBL. Inclusions of other particle types, such as soot, in sea-salt particles might also enhance the reactivity of halides by mediating the transformation of ozone into more powerful oxidants such as hydroxyl radical. If these enhancements do occur in the environment, they could increase the oxidation of particulate halides (and subsequent release of photoreactive halogens), as well as the oxidation of

particulate S(IV) and organic carbon. However, there are a number of important uncertainties in this suggestion, and evaluating this possible enhancement will require additional laboratory study using more environmentally relevant surfaces and particle types.

Acknowledgements

Funding for this research was provided by the Natural Sciences and Engineering Research Council of Canada (NSERC). Support for C.A. was provided through an NSERC International Postdoctoral Fellowship and the U.S. National Science Foundation (Grant #ATM-9701995). The authors gratefully acknowledge technical assistance from S.-M. Li and D. Toom-Sauntry (Environment Canada), G. Impey (York University), and X.-Y. Tai (York University).

Appendix: Kinetic Model of Bromide Oxidation in Reaction System

The reaction system was modeled as a three-component system consisting of particulate bromide, Br(p), bromide deposited to the flask walls, Br(w), and gas-phase bromine, Br(g). The three processes considered in this system, along with their accompanying first-order rate constants [in brackets], were:

1. Oxidation of particulate bromide: $\mathrm{Br(p)} \rightarrow \mathrm{Br(g)}$ $[k_{\mathrm{P,OX}}]$
2. Deposition of particulate bromide to the walls: $\mathrm{Br(p)} \rightarrow \mathrm{Br(w)}$ $[k_{\mathrm{STICK}}]$
3. Oxidation of wall-deposited bromide: $\mathrm{Br(w)} \rightarrow \mathrm{Br(g)}$ $[k_{\mathrm{W,OX}}]$

We use the term Br(i) (e.g., Br(p) or Br(w)) to refer to the amount of bromide of type i present in the reactor at time t, and the term D{Br(i)} to refer to the cumulative amount of particulate or gaseous bromine collected on the denuder by time t.

Based on this model, the rate of accumulation of wall-deposited bromide is given by

$$\frac{d\mathrm{Br(w)}}{dt} = k_{\mathrm{STICK}}\mathrm{Br(p)} - k_{\mathrm{W,OX}}\mathrm{Br(w)}\,. \tag{A1}$$

Br(p) was approximately constant throughout any given experiment since, at most, only a few percent of Br(p) could be oxidized during the 2 min residence time in the reactor (Section 3.2.2). Thus the rate of bromide deposition to the walls, $R_{\mathrm{Br(w)}} = k_{\mathrm{STICK}}\mathrm{Br(p)}$, is expected to be approximately constant for a given experiment. (The available experimental data provide evidence that this is true.) Integration of Equation (A1) under the assumption that $R_{\mathrm{Br(w)}}$ is constant in a given

experiment yields an expression for Br(w), the amount of wall-deposited bromide at time t:

$$\mathrm{Br(w)} = \frac{R_{\mathrm{Br(w)}}}{k_{\mathrm{W,OX}}}(1 - \mathrm{e}^{-k_{\mathrm{W,OX}}t}) + \mathrm{Br(w,0)}(\mathrm{e}^{-k_{\mathrm{W,OX}}t}), \tag{A2}$$

where Br(w,0) is the amount of bromide deposited to the wall by time zero (defined as the time that ozone exposure started).

From the three processes described at the beginning of the Appendix, the rate of formation of gas phase bromine is represented as

$$R_{\mathrm{Br(g)}} = \frac{d\mathrm{Br(g)}}{dt} = \frac{d\mathrm{D\{Br(g)\}}}{dt} = k_{\mathrm{P,OX}}\mathrm{Br(p)} + k_{\mathrm{W,OX}}\mathrm{Br(w)}. \tag{A3}$$

Note that the rate of collection of gaseous bromine on the denuder is assumed to be equal to its rate of formation since the residence time in the reactor is relatively short. Substitution of Equation (A2) into Equation (A3) modifies this equation to

$$R_{\mathrm{Br(g)}} = k_{\mathrm{P,OX}}\mathrm{Br(p)} + R_{\mathrm{Br(w)}}(1 - \mathrm{e}^{-k_{\mathrm{W,OX}}t}) + k_{\mathrm{W,OX}}\mathrm{Br(w,0)}\mathrm{e}^{-k_{\mathrm{W,OX}}t}. \tag{A4}$$

Integration of Equation (A4) between time zero and time t, assuming that there is no gas phase bromine at time zero, yields an expression for D{Br(g)}, the total amount of gas phase bromine collected by time t:

$$\mathrm{D\{Br(g)\}} = k_{\mathrm{P,OX}}\mathrm{Br(p)}t + R_{\mathrm{Br(w)}}t + \left(\mathrm{Br(w,0)} - \frac{R_{\mathrm{Br(w)}}}{k_{\mathrm{W,OX}}}\right)(1 - \mathrm{e}^{-k_{\mathrm{W,OX}}t}). \tag{A5}$$

As described in the text (Section 3.2.2), it appears that, under our conditions, particulate bromide was an insignificant source of gaseous bromine and that the first term in Equation (A5), $k_{\mathrm{P,OX}}\mathrm{Br(p)}t$, is negligible. Under these conditions D{Br(g)} can be described by

$$\mathrm{D\{Br(g)\}} = R_{\mathrm{Br(w)}}t + \left(\mathrm{Br(w,0)} - \frac{R_{\mathrm{Br(w)}}}{k_{\mathrm{W,OX}}}\right)(1 - \mathrm{e}^{-k_{\mathrm{W,OX}}t}). \tag{A6}$$

Note that $\mathrm{Br(w,0)} = k_{\mathrm{STICK}} \times \mathrm{Br(p)} \times t_{\mathrm{PL}} = R_{\mathrm{Br(w)}} \times t_{\mathrm{PL}}$, where t_{PL} is the particle pre-loading time, i.e., the amount of time that particulate bromide was sent to the flask prior to time zero (defined as the start of ozone exposure). With this, substitution of (A2) into (A6) yields

$$\mathrm{D\{Br(g)\}} + \mathrm{Br(w)} = R_{\mathrm{Br(w)}}(t + t_{\mathrm{PL}}). \tag{A7}$$

Values for $R_{\mathrm{Br(w)}}$ (Tables I and III) were calculated from Equation (A7), i.e., by dividing the total amount of Br(w) and D{Br(g)} accumulated at the end of an experiment by the total amount of time particles were sent to the reaction flask (i.e., pre-loading time plus exposure time). Values for Br(w,0) were calculated by multiplying $R_{\mathrm{Br(w)}}$ by the pre-loading time t_{PL}. With these calculated values of $R_{\mathrm{Br(w)}}$ and Br(w,0), $k_{\mathrm{W,OX}}$ was then determined by solving Equation (A6) with the

experimental data (D{Br(g)}/2 and t) using the 'Curve Fit' routine of SigmaPlot (see Section 3.2.2).

References

Alebic-Juretic, A., Cvitas, T., and Klasinc, L., 1997: Ozone destruction on solid particles, *Environ. Monitor. Assess.* **44**, 241–247.

Allan, B. J., McFiggans, G., Plane, J. M. C., and Coe, H., 2000: Observations of iodine monoxide in the remote marine boundary layer, *J. Geophys. Res.* **105**, 14 363–14 369.

Andreae, M. O., Charlson, R. J., Bruynseels, F., Storms, H., Van Grieken, R., and Maenhaut, W., 1986: Internal mixture of sea salt, silicates, and excess sulfate in marine aerosols, *Science* **232**, 1620–1623.

Behnke, W. and Zetzsch, C., 1989: Smog chamber investigations of the influence of NaCl aerosol on the concentration of O_3 in a photosmog system, in R. D. Bojkov and P. Fabian (eds), *Ozone in the Atmosphere*, A. Deepak Publishing, pp. 519–523.

Behnke, W. and Zetzsch, C., 1990: Heterogeneous production of Cl atoms under simulated tropospheric conditions in a smog chamber, in G. Testelli and G. Angeletti (eds), *Proceedings of the 5th European Symposium on Physico-Chemical Behaviour of Atmospheric Pollutants*, Kluwer, pp. 277–282.

Behnke, W., Scheer, V., and Zetzsch, C., 1995: Production of a photolytic precursor of atomic Cl from aerosols and Cl^- in the presence of O_3, in A. Grimvall and E. W. B. de Leer (eds), *Naturally-Produced Organohalogens*, Kluwer, pp. 375–384.

Braun, W., Herron, J. T., and Kahaner, D. K., 1988: Acuchem: A computer program for modeling complex chemical reaction systems, *Int. J. Chem. Kinetics* **20**, 51–62.

De Haan, D. O., Brauers, T., Oum, K., Stutz, J., Nordmeyer, T., and Finlayson-Pitts, B. J., 1999: Heterogeneous chemistry in the troposphere: Experimental approaches and applications to the chemistry of sea salt particles, *Int. Rev. Phys. Chem.* **18**, 343–385.

Dentener, F. J., Carmichael, G. R., Zhang, Y., Lelieveld, J., and Crutzen, P., 1996: Role of mineral aerosols as a reactive surface in the global troposphere, *J. Geophys. Res.* **101**, 22 869–22 889.

Disselkamp, R. S., Chapman, E. G., Barchet, W. R., Colson, S. D., and Howd, C. D., 1999: BrCl production in NaBr/NaCl/HNO_3/O_3 solutions representative of sea-salt aerosols in the marine boundary layer, *Geophys. Res. Lett.* **26**, 2183–2186.

Fan, S.-M., and Jacob, D. J., 1992: Surface ozone depletion in Arctic spring sustained by bromine reactions on aerosols, *Nature* **359**, 522–524.

Finlayson-Pitts, B. J., Livingston, F. E., and Berko, H. N., 1990: Ozone destruction and bromine photochemistry at ground level in the Arctic spring, *Nature* **343**, 622–625.

Finlayson-Pitts, B. J., 1993: Chlorine atoms as a potential tropospheric oxidant in the marine boundary layer, *Res. Chem. Intermed.* **19**, 235–249.

Foster, K. L., Plastridge, R. A., Bottenheim, J. W., Shepson, P. B., Finlayson-Pitts, B. J., and Spicer, C. W., 2001: The role of Br_2 and BrCl in surface ozone destruction at polar sunrise, *Science* **291**, 471–474.

Fuchs, N. A., 1964: *Mechanics of Aerosols*, translated by R. E. Daisley and M. Fuchs, edited by C. N. Davies, Macmillan, p. 184.

Hamer, W. J. and Wu, Y.-C., 1972: Osmotic coefficients and mean activity coefficients of uni-univalent electrolytes in water at 25 ° C, *J. Phys. Chem. Ref. Data* **1**, 1047–1102.

Hausmann, M. and Platt, U., 1994: Spectroscopic measurement of bromine oxide and ozone in the high Arctic during Polar Sunrise Experiment 1992, *J. Geophys. Res.* **99**, 25 399–25 413.

Heikes, B. G., 1984: Aqueous H_2O_2 production from O_3 in glass impingers, *Atmos. Environ.* **18**, 1433–1445.

Heikes, B. G., Lazrus, A. L., Kok, G. L., Kunen, S. M., Gandrud, B. W., Gitlin, S. N., and Sperry, P. D., 1982: Evidence for aqueous phase hydrogen peroxide synthesis in the troposphere, *J. Geophys. Res.* **87**, 3045–3051.

Hirokawa, J., Onaka, K., Kajii, Y., and Akimoto, H., 1998: Heterogeneous processes involving sodium halide particles and ozone: Molecular bromine release in the marine boundary layer in the absence of nitrogen oxides, *Geophys. Res. Lett.* **25**, 2449–2452.

Hoigné, J., Bader, H., Haag, W. R., and Staehelin, J., 1985: Rate constants of reactions of ozone with organic and inorganic compounds in water – III. Inorganic compounds and radicals, *Water Res.* **19**, 993–1004.

Impey, G. A., Shepson, P. B., Hastie, D. R., Barrie, L. A., and Anlauf, K. G., 1997: Measurements of photolyzable chlorine and bromine during the Polar Sunrise Experiment 1995, *J. Geophys. Res.* **102**, 16 005–16 010.

Jacobson, M. Z., 2001: Strong radiative heating due to the mixing state of black carbon in atmospheric aerosols, *Nature* **409**, 695–697.

Jans, U. and Hoigné, J., 2000: Atmospheric water: Transformation of ozone into OH-radicals by sensitized photoreactions or black carbon, *Atmos. Environ.* **34**, 1069–1085.

Jobson, B. T., Niki, H., Yokouchi, Y., Bottenheim, J., Hopper, F., and Leaitch, R., 1994: Measurements of C_2-C_6 hydrocarbons during the Polar Sunrise 1992 Experiment: Evidence for Cl atom and Br atom chemistry, *J. Geophys. Res.* **99**, 25 355–25 368.

Kamm, S., Möhler, O., Naumann, K.-H., Saathoff, H., and Schurath, U., 1999: The heterogeneous reaction of ozone with soot aerosol, *Atmos. Environ.* **33**, 4651–4661.

Keene, W. C., Maben, J. R., Pszenny, A. A. P., and Galloway, J. N., 1993: Measurement technique for inorganic chlorine gases in the marine boundary layer, *Environ. Sci. Technol.* **27**, 866–874.

Keene, W. C., Jacob, D. J., and Fan, S.-M., 1996: Reactive chlorine – a potential sink for dimethylsulfide and hydrocarbons in the marine boundary layer, *Atmos. Environ.* **30**, i–iii.

Knipping, E. M., Lakin, M. J., Foster, K. L., Jungwirth, P., Tobias, D. J., Gerber, R. B., Dabdub, D., and Finlayson-Pitts, B. J., 2000: Experiments and simulations of ion-enhanced interfacial chemistry on aqueous NaCl aerosols, *Science* **288**, 301–306.

Laux, J. M., Hemminger, J. C., and Finlayson-Pitts, B. J., 1994: X-ray photoelectron spectroscopic studies of the heterogeneous reaction of gaseous nitric acid with sodium chloride – Kinetics and contribution to the chemistry of the marine troposphere, *Geophys. Res. Lett.* **21**, 1623–1626.

Lide, D. R. (ed.), 1999: *CRC Handbook of Chemistry and Physics*, CRC Press, Boca Raton.

Mamou, A., Rabani, J., and Behar, D., 1977: On the oxidation of aqueous Br^- by OH radicals, studied by pulse radiolysis, *J. Phys. Chem.* **81**, 1447–1448.

McFiggans, G., Plane, J. M. C., Allan, B. J., Carpenter, L. J., Coe, H., and O'Dowd, C., 2000: A modeling study of iodine chemistry in the marine boundary layer, *J. Geophys. Res.* **105**, 14 371–14 385.

Michalowski, B. A., Francisco, J. S., Li, S.-M., Barrie, L. A., Bottenheim, J. W., and Shepson, P. B., 2000: A computer model study of multiphase chemistry in the Arctic boundary layer during polar sunrise, *J. Geophys. Res.* **105**, 15 131–15 145.

Mozurkewich, M., 1995: Mechanisms for the release of halogens from sea-salt particles by free radical reactions, *J. Geophys. Res.* **100**, 14 199–14 207.

Niimura, N., Okada, K., Fan, X.-B., Kai, K., Arao, K., and Shi, G.-Y., 1994: A method for the identification of Asian dust-storm particles mixed internally with sea salt, *J. Meteor. Soc. Japan* **72**, 777–784.

Oum, K. W., Lakin, M. J., and Finlayson-Pitts, B. J., 1998a: Bromine activation in the troposphere by the dark reaction of O_3 with seawater ice, *Geophys. Res. Lett.* **25**, 3923–3926.

Oum, K. W., Lakin, M. J., DeHaan, D. O., Brauers, T., and Finlayson-Pitts, B. J., 1998b: Formation of molecular chlorine from the photolysis of ozone and aqueous sea-salt particles, *Science* **279**, 74–77.

Pszenny, A. A. P., Keene, W. C., Jacob, D. J., Fan, S., Maben, J. R., Zetwo, M. P., Springer-Young, M., and Galloway, J. N., 1993: Evidence of inorganic chlorine gases other than hydrogen chloride in marine surface air, *Geophys. Res. Lett.* **20**, 699–702.

Richter, A., Wittrock, F., Eisinger, M., and Burrows, J. P., 1998: GOME observations of tropospheric BrO in northern hemispheric spring and summer 1997, *Geophys. Res. Lett.* **25**, 2683–2686.

Ross, A. B., Mallard, W. G., Helman, W. P., Buxton, G. V., Huie, R. E., and Neta, P., 1998: *NDRL-NIST Solution Kinetics Database: – Ver. 3.0*, Notre Dame Radiation Laboratory, Notre Dame, IN and National Institute of Standards and Technology, Gaithersburg, MD.

Sander, R. and Crutzen, P. J., 1996: Model study indicating halogen activation and ozone destruction in polluted air masses transported to the sea. *J. Geophys. Res.* **101**, 9121–9138.

Seinfeld, J. H. and Pandis, S. N., 1998: *Atmospheric Chemistry and Physics: From Air Pollution to Climate Change*, Wiley, New York.

Spicer, C. W. Chapman, E. G., Finlayson-Pitts, B. J., Plastridge, R. A., Hubbe, J. M., Fast, J. D., and Berkowitz, C. M., 1998: Unexpectedly high concentrations of molecular chlorine in coastal air, *Nature* **394**, 353–356.

Vogt, R., Crutzen, P. J., and Sander, R., 1996: A mechanism for halogen release from sea-salt aerosol in the remote marine boundary layer, *Nature* **383**, 327–330.

Vogt, R., Sander, R., von Glasow, R., and Crutzen, P. J., 1999: Iodine chemistry and its role in halogen activation and ozone loss in the marine boundary layer: A model study, *J. Atmos. Chem.* **32**, 375–395.

von Gunten, U. and Hoigné, J., 1994: Bromate formation during ozonation of bromide-containing waters: Interaction of ozone and hydroxyl radical reactions, *Environ. Sci. Technol.* **28**, 1234–1242.

Wardman, P., 1989: Reduction potentials of one-electron couples involving free radicals in aqueous solution, *J. Phys. Chem. Ref. Data* **18**, 1637–1755.

Weast, R. C. (ed.), 1981: *CRC Handbook of Chemistry and Physics*, CRC Press, Boca Raton.